Closed-Form Conversion Between Mean and Osculating Elements in Vectorial Form

Martin Lara

January 18, 2024

(Preprint) SciTech 2023-078

CLOSED-FORM CONVERSION BETWEEN MEAN AND OSCULATING ELEMENTS IN VECTORIAL FORM

Martin Lara*

For the zonal part of the gravitational potential, the closed-form conversion between mean and osculating variables is derived from a generating function up to an arbitrary degree. We show that this scalar generator can be constructed directly in vectorial elements. At difference from alternative solutions in the literature, the closed-form generating function is forced to be purely periodic by the appropriate determination of the arbitrary integration function that is inherent to the procedure. By providing also the frozen-orbit condition for the vectorial case, two relevant facts of the frozen orbits solutions are clearly highlighted. Namely, the rotating-frame nature of frozen orbits and the need of a purely short-period conversion to establish the equivalence between frozen orbits and periodic orbits in the orbital plane.

INTRODUCTION

The traditional decomposition of perturbed Keplerian motion into secular, long- and short-period effects, shows the dominance of the zonal harmonics terms of the gravitational potential in the long-term evolution of non-resonant orbits of artificial-satellite theory.[1–3] On average, the zonal model yields a coupled differential system in the eccentricity and argument of the periapsis, whose stationary solutions disclose a noteworthy class of orbits for their application to a variety of missions. Namely, the orbits with frozen periapsis and almost constant eccentricity, which are customarily denoted as *frozen orbits*.

Beyond the traditional truncation of the gravitational potential to the zonal harmonics of the second and third degree, customarily used in the preliminary design of mapping orbits,[4–6] the frozen orbit design may require much higher order truncations of the zonal potential,[7,8] which, besides, disclose important qualitative changes in the frozen orbits' dynamics.[9,10] Still, since typical mapping orbits have low eccentricities, truncation to the lower powers of the eccentricity eases the computation of general expressions for the frozen orbit condition.[11–13] Alternatively, the condition for steady-state eccentricity can be obtained in closed form, in this way reducing the computational burden, on the one hand, and extending the application of the theory to the case of high-eccentricity orbits, on the other hand. Explicit expressions computed by brut-force are, of course, permitted, but may make software development troublesome due to the need of programming additional code for each new term required. Rather, available recursion formulas that allow for dealing with an arbitrary number of zonal harmonics—based on either Kaula's linear theory[2,3] or the method of Lie transforms[14,15]—allow for a much efficient software implementation.[16,17] While the methods of Kaula and the Lie transforms yield equivalent results regarding the mean-element dynamics in

*Scientific Computing and Technological Innovation Center, University of La Rioja, Edificio CCT, C/ Madre de Dios, 53, ES-26006 Logroño, Spain

the linear approximation, the way of arranging the solution is fundamental in the implementation of the linear theory as computer code, in which case Kaula's efficient recursions have been reported to provide clearly advantages.[18]

The time average of the gravitational potential, or a disturbing function in general, that yields the long-term dynamics is mathematically supported by a transformation from mean to osculating elements.[19,20] This connection between the mean and osculating dynamics is important for orbit monitoring too,[21] as well as for maneuver planning,[22,23] in which case full gravitational models may be needed in the conversion between osculating and mean elements in order to meet accuracy requirements of particular missions.[24,25] Existing algorithms achieving the conversion between osculating and mean elements based on either Kaula's or the Lie transform approach, rely on the usual expansions of the elliptic motion,[26,27] yet such conversion can be achieved in closed form when constraining to the zonal part of the gravitational potential. In particular, the generating function of the mean to osculating transformation has been computed by the method of Lie transforms in Ref. 17. However, the fact that this generating function is computed in Delaunay variables may cause trouble in the evaluation of the transformation equations it spawns due to the singularity of these variables for circular orbits. On the other hand, it is known that vectorial formulations of the variation equations, while redundant, enjoy real merits. This is not only due to their non-singular character as well as the symmetry they provide to the variation equations,[28–30] but also for the stability of numerical integrations based on them.[31]

We take advantage of the vectorial approach, and derive the generating function of the mean to osculating transformation of the zonal potential in vectorial form, yet constrained to the linear terms. More precisely, we present it in terms of the eccentricity vector and the usual non-dimensional version of the angular momentum vector, a set of non-singular elements that is sometimes termed as the Milankovitch variables.[32–35] To be complete, we also derive the frozen orbit condition in the same set of vectorial variables, which, to our knowledge, is missing in the literature.

The linear theory is adequate for almost spherical bodies, like Venus or the Moon. However, second order effects of the zonal harmonic of degree two are needed in the case of artificial-satellite orbits of Earth-like planets. While these effects are taken into account in classical analytical orbit theories,[36–38] the computations of mean elements from them requires iterative procedures.[39–41] On the contrary, the explicit osculating-to-mean transformation is readily derived with the method of Lie transforms. Because the relevant higher-order effects commonly constrain to the contribution of a single zonal harmonic, these additional terms, when needed, are simply added to the linear theory from available expressions in the literature, which, besides, can be limited to the short-period corrections of the semimajor axis.[42–44]

The inclusion of additional effects stemming from the three-body dynamics is most times required for realistic mission orbit design.[45–52] In that case, the generating function must be supplemented with the additional terms considered in the perturbation model. Beyond particular, low-degree truncations of the third-body disturbing potential commonly discussed in the literature,[35,53–55] the vectorial formulation of third-body perturbations up to an arbitrary degree has been thoroughly discussed in Ref. 56, from which specific terms can be directly borrowed when needed.

ZONAL POTENTIAL WITHOUT PARALLACTIC TERMS

The gravitational potential is usually derived from Laplace's equation in terms of the spherical variables (r, φ, λ), denoting the distance, latitude and longitude, respectively. For spheroidal bodies, the potential is constrained to the contribution of the zonal harmonics, which do not depend on longitude.[57,58] Thus,

$$V = -\frac{\mu}{r} + U(r,\varphi), \tag{1}$$

in which μ denotes the gravitational parameter, and the disturbing zonal potential is

$$U = \frac{\mu}{r}\sum_{i\geqslant 2}\frac{R_\oplus^i}{r^i}J_i P_i(\sin\varphi), \tag{2}$$

where $R_\oplus$ is the equatorial radius of the attracting body, J_i are the zonal harmonic coefficients of the gravitational potential, and P_i denote the Legendre polynomial of degree i.

Potential functions involving only Legendre polynomials can be efficiently handled in closed form in the search for perturbation solutions to orbital motion problems.[9,56] In that cases, the closed-form approach is eased by replacing the parallactic terms $(p/r)^m$, with p denoting the pericenter distance and $m \geqslant 3$, in terms of the Keplerian orbital elements $(a, e, I, \Omega, \omega, M)$—denoting semimajor axis, eccentricity, inclination, right ascension of the ascending node, argument of the periapsis, and mean anomaly, respectively— while keeping the term $(p/r)^2$ as a factor.[18,31] This factor is left out of the summation in Eq. (2), in preparation for a following closed form integration based on the differential relation between the true anomaly f and mean one

$$\mathrm{d}M = \frac{n}{\Theta}r^2\,\mathrm{d}f = \frac{r^2}{p^2}\eta^3\,\mathrm{d}f, \tag{3}$$

in which $n = \sqrt{\mu/a^3} = \Theta\eta^3/p^2$ denotes the mean motion, Θ is the specific angular momentum, $p = a\eta^2$ and $\eta = (1-e^2)^{1/2}$.

More precisely, in a way similar to Ref. 3, the disturbing potential in Eq. (2) is written it in the form[18]

$$U = \frac{\mu}{a}\frac{p^2}{r^2}\frac{1}{\eta^3}\sum_{i\geqslant 2}J_i V_i, \tag{4}$$

in which

$$V_i = \frac{R_\oplus^i}{p^i}\eta\left(\frac{p}{r}\right)^{i-1}P_i(\sin\varphi). \tag{5}$$

Replacing $\sin\varphi = \sin I\sin(f+\omega)$, the Legendre polynomials are conveniently written in terms of the orbital elements using Kaula's inclination functions,[3] which admit efficient recursive computation.[59,60] However, these functions are not adequate in the reformulation of the zonal potential in vectorial elements, which is rather written in the form[31]

$$V_i = \frac{1}{2^i}\frac{R_\oplus^i}{p^i}\eta\sum_{j=0}^{i-1}\sum_{l=0}^{\lfloor\frac{i}{2}\rfloor}\sum_{m=0}^{i-2l}\binom{i-1}{j}\binom{i}{l}\binom{2i-2l}{i}\binom{i-2l}{m}(-1)^l e^j k_1^m k_2^{i-m-2l}\Psi_{i,j,l,m}(f), \tag{6}$$

where

$$\Psi_{i,j,l,m} = \cos^{j+m} f\sin^{i-m-2l} f. \tag{7}$$

are trigonometric functions of the true anomaly only, the operator $\lfloor\ \rfloor$ denotes the integer part of the argument, and k_i, $i = 1, 2, 3$, denote the direction cosines of the unit vector defining the equatorial plane $\boldsymbol{k}$ in the apsidal frame. The later is defined by the directions of the instantaneous eccentricity vector $\hat{\boldsymbol{e}}$, the normal to orbital plane $\boldsymbol{n}$, and $\boldsymbol{b} = \boldsymbol{n} \times \hat{\boldsymbol{e}}$, thus completing a direct frame $(\hat{\boldsymbol{e}}, \boldsymbol{b}, \boldsymbol{n})$. In this frame, $\boldsymbol{k} = R_3(\omega)R_1(I)(0,0,1)^T$, where R_1, R_2, and R_3 denote the usual rotation matrices, and the superindex T denotes transposition. That is,

$$\begin{pmatrix} k_1 \\ k_2 \\ k_3 \end{pmatrix} \equiv \begin{pmatrix} \hat{\boldsymbol{e}} \cdot \boldsymbol{k} \\ \boldsymbol{b} \cdot \boldsymbol{k} \\ \boldsymbol{n} \cdot \boldsymbol{k} \end{pmatrix} = \begin{pmatrix} \sin I \sin\omega \\ \sin I \cos\omega \\ \cos I \end{pmatrix}. \tag{8}$$

For later manipulation, the trigonometric functions $\Psi_{i,j,l,m}(f)$ are conveniently written as Fourier series using standard relations between circular functions and exponentials, from which we readily obtain

$$\cos^\kappa f \sin^\sigma f = \frac{(-1)^{\frac{\sigma-\sigma^\star}{2}}}{2^{\kappa+\sigma}} \sum_{q=0}^{\sigma} (-1)^q \binom{\sigma}{q} \sum_{k=0}^{\kappa} \binom{\kappa}{k} \cos\left[(\kappa+\sigma-2k-2q)f - \tfrac{\pi}{2}\sigma^\star\right], \tag{9}$$

where $\sigma^\star \equiv \sigma \bmod 2$. Hence,

$$\Psi_{i,j,l,m} = \frac{(-1)^{\frac{i-m-\sigma^\star}{2}-l}}{2^{j+i-2l}} \sum_{q=0}^{i-m-2l} (-1)^q \binom{i-m-2l}{q} \sum_{k=0}^{j+m} \binom{j+m}{k} \times \cos\left[(j+i-2l-2k-2q)f - \tfrac{\pi}{2}\sigma^\star\right], \tag{10}$$

where, now, $\sigma^\star = (i-m) \bmod 2$. Moreover, the constraint $k_1^2 + k_2^2 + k_3^2 = 1$ jointly with the use of the binomial theorem, allows us to write

$$k_2^{2\kappa} = (1 - k_3^2 - k_1^2)^\kappa = \sum_{t=0}^{\kappa} \binom{\kappa}{t} (-1)^t k_1^{2t} (1-k_3^2)^{\kappa-t}. \tag{11}$$

Therefore, Eq. (6) is rewritten as

$$V_i = \frac{1}{2^i} \frac{R_\oplus^i}{p^i} \eta \sum_{j=0}^{i-1} \sum_{l=0}^{\lfloor\frac{i}{2}\rfloor} \sum_{m=0}^{i-2l} \sum_{t=0}^{\lfloor\frac{i-m-2l}{2}\rfloor} B_{i,j,l,m,t} e^j k_1^{m+2t} (1-k_3^2)^{\frac{i-m}{2}-l-t} \Psi_{i,j,l,m}(f), \tag{12}$$

where, for abbreviation in printed expressions, we introduce the numeric coefficients

$$B_{i,j,l,m,t} = \binom{i-1}{j} \binom{i}{l} \binom{2i-2l}{i} \binom{i-2l}{m} \binom{\lfloor\frac{i-m-2l}{2}\rfloor}{t} (-1)^{l+t}. \tag{13}$$

Replacing $k_1 \equiv \boldsymbol{k} \cdot \hat{\boldsymbol{e}}$, $k_3 \equiv \boldsymbol{k} \cdot \boldsymbol{n}$, from Eq. (8), and introducing the nondimensional vectors $\boldsymbol{e} = e\hat{\boldsymbol{e}}$, and $\boldsymbol{\eta} = \eta\boldsymbol{n}$, we provide Eq. (12) with a complete vectorial character $V_i = V_i(\boldsymbol{e}, \boldsymbol{\eta}, f)$. Thus,

$$V_i = \frac{1}{2^i} \frac{R_\oplus^i}{a^i} \sum_{j=0}^{i-1} \sum_{l=0}^{\lfloor\frac{i}{2}\rfloor} \sum_{m=0}^{i-2l} \sum_{t=0}^{\tilde{t}} B_{i,j,l,m,t} \frac{e^{j-m-2t}}{\eta^{2i-1}} (\boldsymbol{e} \cdot \boldsymbol{k})^{m+2t} \left[1 - \frac{(\boldsymbol{\eta} \cdot \boldsymbol{k})^2}{\eta^2}\right]^{\frac{i-m-2l-2t}{2}} \Psi_{i,j,l,m}(f), \tag{14}$$

cf. Ref. 31. It goes without saying that because Eq. (12) is free from divisions by the eccentricity, Eq. (14) must also be free from these kinds of divisors. Then, the maximum value of the summation index t in Eq. (14) is constrained to the value $\tilde{t} = \min(i-2l, j-2t)$, to avoid the need of a post processing in order to remove spurious eccentricity denominators introduced by possible negative values of the exponent $j-m-2t$ of $e = \sqrt{\boldsymbol{e} \cdot \boldsymbol{e}}$.

THE LONG-TERM VARIATIONS AND THE FROZEN ORBIT CONDITION

The vectorial form of Eq. (14) is useful in computing the averaged disturbing potential $\langle U\rangle_M = \frac{1}{2\pi}\int_0^{2\pi} U(M)\,\mathrm{d}M$ from Eq. (4). Namely, using the differential relation in Eq. (3),

$$\langle U\rangle_M = \langle (r/p)^2\eta^3 U\rangle_f = \frac{\mu}{a}\sum_{i\geqslant 2} J_i\langle V_i\rangle_f, \tag{15}$$

where

$$\langle V_i\rangle_f = \frac{1}{2^i}\frac{R_\oplus^i}{a^i}\sum_{j=0}^{i-1}\sum_{l=0}^{\lfloor\frac{i}{2}\rfloor}\sum_{m=0}^{i-2l}\sum_{t=0}^{\tilde t} B_{i,j,l,m,t}\frac{e^{j-m-2t}}{\eta^{2i-1}}(\boldsymbol{e}\cdot\boldsymbol{k})^{m+2t}\left[1-\frac{(\boldsymbol{\eta}\cdot\boldsymbol{k})^2}{\eta^2}\right]^{\frac{i-m-2l-2t}{2}}\langle\Psi_{i,j,l,m}\rangle_f. \tag{16}$$

The average of the trigonometric terms over the true anomaly is readily obtained from Eq. (10) by noting that all of them vanish save those in which $q = \frac{1}{2}(j+i)-l-k$. Namely,

$$\langle\Psi_{i,j,l,m}\rangle_f = \frac{(-1)^{\frac{j+m}{2}}}{2^{j+i-2l}}\sum_{k=0}^{j+m}(-1)^k\binom{i-m-2l}{\frac{j+i}{2}-l-k}\binom{j+m}{k}. \tag{17}$$

It is worth noticing that the numeric coefficients $\langle\Psi_{i,j,l,m}\rangle_f$ only depend on two indices, which, besides, must be even. Indeed, $\langle\Psi_{i,j,l,m}\rangle_f = \Xi_{i-m-2l,j+m}$ where

$$\Xi_{\alpha,\beta} = \frac{(-1)^{\frac{1}{2}\alpha}}{4^{\frac{\alpha+\beta}{2}}}\sum_{k=0}^{\alpha}\binom{\beta}{\frac{\alpha+\beta}{2}-k}\binom{\alpha}{k}(-1)^k, \tag{18}$$

with even indices α and β.

The averaging process has removed any dependence of the disturbing function on the mean anomaly, with the result of making constant, on average, the semimajor axis. Thus $L = \sqrt{\mu a}$ is an integral of the averaged problem which may be used to scale the disturbing function. When done, we can set the mean variations of the non-dimensional, vectorial elements $\boldsymbol{\eta}$ and $\boldsymbol{e}$ in in a neat symmetric form that is hailed regarding their numerical integration.[31,32,34] For the zonal potential of concern, we borrow the vectorial variations from Ref. 31, which we rather set in the slow scale $\tau = nt$. Thus,

$$\frac{\mathrm{d}\boldsymbol{\eta}}{\mathrm{d}\tau} = \frac{1}{\eta}\sum_{i\geqslant 2}\frac{J_i}{2^i}\frac{R_\oplus^i}{p^i}\left[(\boldsymbol{\eta}\cdot\boldsymbol{k})(\boldsymbol{\eta}\times\boldsymbol{k})\gamma_i - \eta^2(\boldsymbol{e}\times\boldsymbol{k})\rho_i\right], \tag{19}$$

$$\frac{\mathrm{d}\boldsymbol{e}}{\mathrm{d}\tau} = \frac{1}{\eta}\sum_{i\geqslant 2}\frac{J_i}{2^i}\frac{R_\oplus^i}{p^i}\left[(\boldsymbol{\eta}\cdot\boldsymbol{k})(\boldsymbol{e}\times\boldsymbol{k})\gamma_i - \eta^2(\boldsymbol{\eta}\times\boldsymbol{k})\rho_i - (\boldsymbol{\eta}\times\boldsymbol{e})\rho_{i+1}\right], \tag{20}$$

where the symbol $\times$ denotes the cross product, whereas

$$\begin{aligned}\gamma_i = {} & 2\sum_{l=0}^{\lfloor i/2\rfloor-1}\sum_{q=l+1}^{\lfloor i/2\rfloor}\sum_{m=l+1}^{q}\binom{i}{l}\binom{2i-2l}{i}\binom{i-2l}{i-2q}\binom{q-l}{q-m}(-1)^{l+q-m}(m-l)\\ & \times\left[1-(\boldsymbol{\eta}\cdot\boldsymbol{k})^2/\eta^2\right]^{m-l-1}(\boldsymbol{e}\cdot\boldsymbol{k})^{i-2m}Q_{i,i-m,q-l,q}(\boldsymbol{e}\cdot\boldsymbol{e}),\end{aligned} \tag{21}$$

$$\rho_i = \sum_{l=0}^{\lfloor i/2\rfloor}\sum_{q=l}^{\lfloor i/2\rfloor}\sum_{m=l}^{q}\binom{i}{l}\binom{2i-2l}{i}\binom{i-2l}{i-2q}\binom{q-l}{q-m}(-1)^{l+q-m}(i-2m)$$

$$\times [1-(\boldsymbol{\eta}\cdot\boldsymbol{k})^2/\eta^2]^{m-l}(\boldsymbol{e}\cdot\boldsymbol{k})^{i-2m-1}Q_{i,i-m,q-l,q}(\boldsymbol{e}\cdot\boldsymbol{e}), \tag{22}$$

in which

$$Q_{i,i-m,q-l,q} = \sum_{j=i-m}^{i-1}\binom{i-1}{2j-i}\Xi_{2(j-q),2(q-l)}(\boldsymbol{e}\cdot\boldsymbol{e})^{j-i+m}, \tag{23}$$

are eccentricity polynomials. Remark that both $\boldsymbol{\eta}\times\boldsymbol{k}$ and $\boldsymbol{e}\times\boldsymbol{k}$ remain in the equatorial plane, and hence $(\mathrm{d}\boldsymbol{\eta}/\mathrm{d}\tau)\cdot\boldsymbol{k}=0$ making the third component of the angular momentum $H=\boldsymbol{G}\cdot\boldsymbol{k}$ an integral. This is just a reflection of the axial symmetry of the original (non-averaged) zonal model, which is not lost in the averaging.

Particular noteworthy solutions to the differential equations (19)–(20) are their equilibria. They would not exist, in general, in inertial space, yet interesting opportunities for mission orbits stem from the dynamics in the orbital plane. That is the remarkable case of frozen orbits, whose eccentricity vectors remain fixed in the nodal frame. Therefore, we reformulate the mean variations in the rotating, nodal frame and investigate those solutions in which the variation of the eccentricity vector vanishes.

The nodal frame

The nodal frame $(O,\boldsymbol{\ell},\boldsymbol{m},\boldsymbol{n})$, is defined by the vectors $\boldsymbol{\ell}=\boldsymbol{k}\times\boldsymbol{n}/\sin I$, where the inclination is obtained from the third of Eq. (8), and $\boldsymbol{m}=\boldsymbol{n}\times\boldsymbol{\ell}$. If, besides, we replace $\boldsymbol{k}$ and $\boldsymbol{e}$ by their projections in the nodal frame, $\boldsymbol{k}=(\boldsymbol{k}\cdot\boldsymbol{n})\boldsymbol{n}+(\boldsymbol{k}\cdot\boldsymbol{m})\boldsymbol{m}$, and $\boldsymbol{e}=(\boldsymbol{e}\cdot\boldsymbol{\ell})\boldsymbol{\ell}+(\boldsymbol{e}\cdot\boldsymbol{m})\boldsymbol{m}$, straightforward computations turn Eqs. (19)–(20) into

$$\frac{\mathrm{d}\boldsymbol{\eta}}{\mathrm{d}\tau} = \eta\sum_{i\geqslant 2}J_i\frac{R_\oplus^i}{(2p)^i}\left\{-[sc\gamma_i+c(\boldsymbol{e}\cdot\boldsymbol{m})\rho_i]\boldsymbol{\ell}+c(\boldsymbol{e}\cdot\boldsymbol{\ell})\rho_i\boldsymbol{m}-s(\boldsymbol{e}\cdot\boldsymbol{\ell})\rho_i\boldsymbol{n}\right\}, \tag{24}$$

$$\frac{\mathrm{d}\boldsymbol{e}}{\mathrm{d}\tau} = \sum_{i\geqslant 2}J_i\frac{R_\oplus^i}{(2p)^i}\left\{\left[(\boldsymbol{e}\cdot\boldsymbol{m})(c^2\gamma_i+\rho_{i+1})+s\eta^2\rho_i\right]\boldsymbol{\ell}-(\boldsymbol{e}\cdot\boldsymbol{\ell})(c^2\gamma_i+\rho_{i+1})\boldsymbol{m}+cs(\boldsymbol{e}\cdot\boldsymbol{\ell})\gamma_i\boldsymbol{n}\right\}. \tag{25}$$

where

$$s=\boldsymbol{k}\cdot\boldsymbol{m}, \qquad c=\boldsymbol{k}\cdot\boldsymbol{n}, \tag{26}$$

stand for sine and cosine of the inclination, respectively.

From the theorem of the moving frame (Coriolis theorem)

$$\frac{\mathrm{d}\boldsymbol{\eta}}{\mathrm{d}\tau}=\dot{\boldsymbol{\eta}}+\boldsymbol{\omega}\times\boldsymbol{\eta}, \qquad \frac{\mathrm{d}\boldsymbol{e}}{\mathrm{d}\tau}=\dot{\boldsymbol{e}}+\boldsymbol{\omega}\times\boldsymbol{e}, \tag{27}$$

in which overdots mean time differentiation in the rotating frame, and $\boldsymbol{\omega}$ denotes the angular velocity of the nodal frame. That is,

$$\frac{\mathrm{d}}{\mathrm{d}\tau}(\boldsymbol{\ell},\boldsymbol{m},\boldsymbol{n})=\boldsymbol{\omega}\times(\boldsymbol{\ell},\boldsymbol{m},\boldsymbol{n}). \tag{28}$$

Therefore, in order to obtain it, we only need to compute the time variation of the corresponding unit vectors in terms of the perturbation. Thus, first of all, recalling that $\boldsymbol{n}=\boldsymbol{\eta}/\eta$, we compute

$$\frac{\mathrm{d}\boldsymbol{n}}{\mathrm{d}\tau}=\frac{1}{\eta}\frac{\mathrm{d}\boldsymbol{\eta}}{\mathrm{d}\tau}-\frac{1}{\eta}\frac{\mathrm{d}\eta}{\mathrm{d}\tau}\boldsymbol{n}, \tag{29}$$

where the variation of $\boldsymbol{\eta}$ is given in Eq. (24). The, from the preservation of the third component of the angular momentum H jointly with the preservation of L, on average, $H/L = \eta\cos I$ remains constant, and hence

$$\frac{1}{\eta}\frac{\mathrm{d}\eta}{\mathrm{d}\tau} = -\frac{1}{c}\frac{\mathrm{d}c}{\mathrm{d}\tau} = \frac{s}{c^2}\frac{\mathrm{d}s}{\mathrm{d}\tau}. \tag{30}$$

Analogously, replacing $\boldsymbol{\ell} = \boldsymbol{k}\times\boldsymbol{n}/s$ and taking Eq. (29) into account, we obtain

$$\frac{\mathrm{d}\boldsymbol{\ell}}{\mathrm{d}\tau} = \frac{1}{s}\boldsymbol{k}\times\frac{\mathrm{d}\boldsymbol{n}}{\mathrm{d}\tau} - \frac{1}{s}\frac{\mathrm{d}s}{\mathrm{d}\tau}\boldsymbol{\ell} = \frac{1}{s}\frac{1}{\eta}\boldsymbol{k}\times\frac{\mathrm{d}\boldsymbol{\eta}}{\mathrm{d}\tau} - \frac{1}{s}\frac{1}{c^2}\frac{\mathrm{d}s}{\mathrm{d}\tau}\boldsymbol{\ell}$$

in which we further replace Eq. (24), to obtain

$$\frac{\mathrm{d}\boldsymbol{\ell}}{\mathrm{d}\tau} = (s\boldsymbol{n} - c\boldsymbol{m})\frac{c}{s}\sum_{i\geqslant 2} J_i\frac{R_\oplus^i}{(2p)^i}[s\gamma_i + \rho_i(\boldsymbol{e}\cdot\boldsymbol{m})] - \frac{1}{sc}\left[\frac{\mathrm{d}I}{\mathrm{d}\tau} + c\sum_{i\geqslant 2} J_i\frac{R_\oplus^i}{(2p)^i}\rho_i(\boldsymbol{e}\cdot\boldsymbol{\ell})\right]\boldsymbol{\ell}, \tag{31}$$

where the last term must vanish because $\boldsymbol{\ell}$ is a unit vector, whose variation must be orthogonal to itself. In this way we obtain the first component of $\boldsymbol{\omega}$ in the nodal frame $\boldsymbol{\omega}\cdot\boldsymbol{\ell} = \mathrm{d}I/\mathrm{d}\tau$.

Replacing Eq. (24) analogously in Eq. (29) yields

$$\frac{\mathrm{d}\boldsymbol{n}}{\mathrm{d}\tau} = \sum_{i\geqslant 2} J_i\frac{R_\oplus^i}{(2p)^i}c\left\{\rho_i(\boldsymbol{e}\cdot\boldsymbol{\ell})\boldsymbol{m} - [s\gamma_i + \rho_i(\boldsymbol{e}\cdot\boldsymbol{m})]\,\boldsymbol{\ell}\right\} - \frac{s}{c}\left[\frac{\mathrm{d}I}{\mathrm{d}\tau} + c\sum_{i\geqslant 2} J_i\frac{R_\oplus^i}{(2p)^i}\rho_i(\boldsymbol{e}\cdot\boldsymbol{\ell})\right]\boldsymbol{n}, \tag{32}$$

with the same comment as before regarding the last term on the right side of the equation.

From Eqs. (28), (31), and (32), we easily identify the rotation induced by the zonal perturbation on the nodal frame. Namely,

$$\boldsymbol{\omega} = -c\sum_{i\geqslant 2} J_i\frac{R_\oplus^i}{(2p)^i}\left\{(\boldsymbol{e}\cdot\boldsymbol{\ell})\rho_i\boldsymbol{\ell} + [s\gamma_i + (\boldsymbol{e}\cdot\boldsymbol{m})\rho_i]\,\boldsymbol{m} + \frac{c}{s}[s\gamma_i + (\boldsymbol{e}\cdot\boldsymbol{m})\rho_i]\,\boldsymbol{n}\right\}. \tag{33}$$

Frozen orbits

After solving Eq. (27) for the variations in the moving frame, we compute

$$\boldsymbol{\omega}\times\boldsymbol{\eta} = \eta(\boldsymbol{\omega}\cdot\boldsymbol{m})\boldsymbol{\ell} - \eta(\boldsymbol{\omega}\cdot\boldsymbol{\ell})\boldsymbol{m}, \tag{34}$$

$$\boldsymbol{\omega}\times\boldsymbol{e} = -(\boldsymbol{e}\cdot\boldsymbol{m})(\boldsymbol{\omega}\cdot\boldsymbol{n})\boldsymbol{\ell} + (\boldsymbol{e}\cdot\boldsymbol{\ell})(\boldsymbol{\omega}\cdot\boldsymbol{n})\boldsymbol{m} + [(\boldsymbol{e}\cdot\boldsymbol{m})(\boldsymbol{\omega}\cdot\boldsymbol{\ell}) - (\boldsymbol{e}\cdot\boldsymbol{\ell})(\boldsymbol{\omega}\cdot\boldsymbol{m})]\boldsymbol{n}, \tag{35}$$

from Eq. (33), and combine them with the variations in the inertial frame in Eqs. (24) and (25), respectively. We finally obtain

$$\dot{\boldsymbol{\eta}} = -s\eta(\boldsymbol{e}\cdot\boldsymbol{\ell})\sum_{i\geqslant 2} J_i\frac{R_\oplus^i}{(2p)^i}\rho_i\boldsymbol{n},$$

$$\dot{\boldsymbol{e}} = \frac{1}{s}\sum_{i\geqslant 2} J_i\frac{R_\oplus^i}{(2p)^i}\left\{\rho_i s^2\eta^2\boldsymbol{\ell} + [s\rho_{i+1} - c^2(\boldsymbol{e}\cdot\boldsymbol{m})\rho_i][(\boldsymbol{e}\cdot\boldsymbol{m})\boldsymbol{\ell} - (\boldsymbol{e}\cdot\boldsymbol{\ell})\boldsymbol{m}]\right\},$$

which show that the variation of $\boldsymbol{\eta}$ identically vanishes in the particular case in which $\boldsymbol{e}\cdot\boldsymbol{\ell} = 0$, that is $\omega = \pm\frac{\pi}{2}$ and $\boldsymbol{e}\cdot\boldsymbol{m} = \pm e$. In that case,

$$\dot{\boldsymbol{e}}(\omega = \pm\tfrac{\pi}{2}) = \frac{1}{s}\sum_{i\geqslant 2} J_i\frac{R_\oplus^i}{(2p)^i}\left[(s^2 - e^2)\rho_i + s(\boldsymbol{e}\cdot\boldsymbol{m})\rho_{i+1}\right]\boldsymbol{\ell} \tag{36}$$

where the functions ρ_i must also be evaluated for the value $\omega = \pm\frac{\pi}{2}$, which yields $\boldsymbol{e}\cdot\boldsymbol{k} = \pm es$, respectively. Therefore, we can replace $s(\boldsymbol{e}\cdot\boldsymbol{m}) = \boldsymbol{e}\cdot\boldsymbol{k} \equiv e_k$ in this particular case, and the frozen orbit condition is constrained to the single equation ($s \neq 0$)

$$0 = \sum_{i\geqslant 2} J_i \frac{R_\oplus^i}{(2p)^i}\left[(s^2 - e^2)\rho_i + e_k\rho_{i+1}\right], \qquad \rho_k = \rho_k(e^2, e_k, s^2), \tag{37}$$

which is non-singular save for the case of rectilinear orbits, and was computed in closed-form. Recall that, in our vectorial notation, $s^2 = 1 - (\boldsymbol{\eta}\cdot\boldsymbol{k})^2/\eta^2$, $\eta^2 = 1 - e^2$, $e^2 = \boldsymbol{e}\cdot\boldsymbol{e}$, and $e_k = \boldsymbol{e}\cdot\boldsymbol{k}$.

The implicit form of Eq. (37), $F(e, s; \omega = \pm\frac{\pi}{2}, a) = 0$ represents two curves $e = e(I; \omega = \pm\frac{\pi}{2})$ in the parameter line $a = a_0$, which provide immediate insight into the frozen orbits geometry in a global context by means of the depiction of inclination-eccentricity diagrams. Still, these diagrams lack of stability information, which must be locally investigated. This can be done graphically as well, by representing contour plots of the averaged potential (15) in the parameters plane $(L = L_0, H = H_0)$. The reduced phase space is the sphere, and hence usual projections in the cylindrical map provided by the (mean) variables (e, ω) miss circular obits. The local flow in the close vicinity of circular orbits is more suitably displayed through projections on the $(e\cos\omega, e\sin\omega)$ plane, in the alternative parameters plane $a_0 = L_0^2/\mu$, $\cos I_{\text{circular}} = H_0/L_0$.

GENERATING FUNCTION AND NON-SINGULAR SHORT-PERIOD CORRECTIONS

The insight on the long-term dynamics provided by the averaging carried out in the previous section is mathematically supported by a transformation from osculating to mean variables. Moreover, the Hamiltonian nature of the zonal problem permits to derive this transformation from a scalar generating function $\mathcal{W} = \sum_{j\geqslant 0}(\epsilon/j!)^j\mathcal{W}_{j+1}$.[15] To first order effects, the periodic terms needed in the conversion between mean and osculating variables of a function $\mathcal{F}$ of the chosen canonical set of variables are obtained as $\Delta = \{\mathcal{F}; \mathcal{W}_1\}$. The mean to osculating transformation is then $\mathcal{F} = \mathcal{F}' + \epsilon\Delta|_{\text{mean}}$ whereas the osculating-to-mean transformation $\mathcal{F}' = \mathcal{F} - \epsilon\Delta$.

The needed term of the generating function is computed as

$$\mathcal{W}_1 = \frac{1}{n}\int (U - \langle U\rangle_M)\,\mathrm{d}M, \tag{38}$$

which is determined up to an arbitrary function $\mathcal{C}$ with the only condition of being free from the mean anomaly.[61–63] That is, $\mathrm{d}\mathcal{C}/\mathrm{d}M = 0$. The closed-form integration is obtained with the help of the differential relation in Eq. (3), which is replaced into Eq. (38) to obtain

$$\mathcal{W}_1 = -\frac{1}{n}\langle U\rangle_M M + \frac{1}{n}\int \frac{r^2}{p^2}\eta^3 U\,\mathrm{d}f = \frac{1}{n}\langle U\rangle_M\phi + \frac{1}{n}\int\left(\frac{r^2}{p^2}\eta^3 U - \langle U\rangle_M\right)\mathrm{d}f,$$

where $\phi = f - M$ denotes the equation of the center. Replacing U and $\langle U\rangle_M$ from Eqs. (4) and (15), respectively, we obtain

$$\mathcal{W}_1 = \Theta\frac{\phi}{\eta}\sum_{i\geqslant 2} J_i\langle V_i\rangle_f + \Theta\frac{1}{\eta}\sum_{i\geqslant 2} J_i\int V_i^*(f)\,\mathrm{d}f, \tag{39}$$

where $V_i^* = V_i - \langle V_i\rangle_f$ comprises the terms of V_i that are purely periodic in f. More precisely, the integration of V_i^* is obtained by simply excluding from Eq. (12) the terms of the summation in

Eq. (10) with index $q = q^* \equiv \frac{1}{2}(j+i) - l - k$. Thus,

$$V_i^* = \frac{1}{2^i}\frac{R_\oplus^i}{p^i}\eta\sum_{j=0}^{i-1}\sum_{l=0}^{\lfloor\frac{i}{2}\rfloor}\sum_{m=0}^{i-2l}\sum_{t=0}^{\lfloor\frac{i-m-2l}{2}\rfloor} B_{i,j,l,m,t}e^j k_1^{m+2t}(1-k_3^2)^{\frac{i-m}{2}-l-t}\Psi_{i,j,l,m}^*(f), \tag{40}$$

where

$$\Psi_{i,j,l,m}^* = \frac{(-1)^{\frac{i-m-\sigma^\star}{2}-l}}{2^{j+i-2l}}\sum_{\substack{q=0\\q\neq q^*}}^{i-m-2l}(-1)^q\binom{i-m-2l}{q}\sum_{k=0}^{j+m}\binom{j+m}{k}\cos\left[2(q^*-q)f - \tfrac{\pi}{2}\sigma^\star\right], \tag{41}$$

and hence,

$$\mathcal{W}_1 = \frac{\Theta}{\eta}\phi\sum_{i\geqslant 2}J_i\langle V_i\rangle_f + \frac{\Theta}{\eta}\sum_{i\geqslant 2}J_i\frac{1}{2^i}\frac{R_\oplus^i}{p^i}\eta\sum_{j=0}^{i-1}\sum_{l=0}^{\lfloor\frac{i}{2}\rfloor}\sum_{m=0}^{i-2l}\sum_{t=0}^{\lfloor\frac{i-m-2l}{2}\rfloor} B_{i,j,l,m,t}e^j k_1^{m+2t}(1-k_3^2)^{\frac{i-m}{2}-l-t}$$
$$\times\frac{(-1)^{\frac{i-m-\sigma^\star}{2}-l}}{2^{j+i-2l}}\sum_{\substack{q=0\\q\neq q^*}}^{i-m-2l}(-1)^q\binom{i-m-2l}{q}\sum_{k=0}^{j+m}\binom{j+m}{k}\frac{\sin\left[2(q^*-q)f-\frac{\pi}{2}\sigma^\star\right]}{2(q^*-q)} + \mathcal{C}. \tag{42}$$

Remark that, in order to $\mathcal{W}_1$ be purely periodic in the mean anomaly, we must choose a nonvanishing integration constant $\mathcal{C}$.[62,64,65] Indeed, taking into account that the equation of the center averages to zero, and that[66]

$$\frac{1}{2\pi}\int_0^{2\pi}\sin(mf+\xi)\,\mathrm{d}M = \left(\frac{-e}{1+\eta}\right)^m(1+m\eta)\sin\xi,$$

in order to guarantee that $\mathcal{W}_1$ is purely periodic in the mean anomaly, that is $\langle\mathcal{W}_1\rangle_M = 0$, we must choose

$$\mathcal{C} = -\frac{\Theta}{\eta}\sum_{i\geqslant 2}J_i\frac{1}{2^i}\frac{R_\oplus^i}{p^i}\eta\sum_{j=0}^{i-1}\sum_{l=0}^{\lfloor\frac{i}{2}\rfloor}\sum_{m=0}^{i-2l}\sum_{t=0}^{\lfloor\frac{i-m-2l}{2}\rfloor} B_{i,j,l,m,t}e^j k_1^{m+2t}(1-k_3^2)^{\frac{i-m}{2}-l-t}\frac{(-1)^{\frac{i+m+1}{2}+l+j}}{2^{j+i-2l}}$$
$$\times\sum_{\substack{q=0\\q\neq q^*}}^{i-m-2l}(-1)^q\binom{i-m-2l}{q}\sum_{k=0}^{j+m}\binom{j+m}{k}\frac{1+2(q^*-q)\eta}{2(q^*-q)}\left(\frac{1-\eta}{1+\eta}\right)^{\frac{j+i}{2}-(l+k+q)}, \tag{43}$$

which only makes sense when $i-m$, and hence $i+m$ is odd.

The use of the function $\mathcal{C}$ allows to establish a connection of frozen orbits and periodic orbits in the orbital plane. Indeed, the former are stationary solution in mean elements which only incorporate short-period effects when translated to osculating elements, and hence their periodic character. Therefore, frozen orbits map onto periodic orbits of the non-averaged model in a suitable reference frame.[67] The connection between these two different kinds of dynamical objects is made through the analytic mean-to-osculating transformation.[68–70] On the other hand, the correspondence between frozen and periodic orbits is necessarily approximate as far as a truncation is involved in the mean elements solution. Higher order truncations, which may be obtained with perturbation methods, would certainly provide a much better approximation of a periodic orbit in the orbital plane in osculating elements.* Still, sooner or later the truncation is unavoidable, and the exact computation of the periodic orbits may require the additional application of differential corrections.[74,75]

EXAMPLE APPLICATION

The newly derived formulas have been validated by comparison with alternative expressions in the literature,[75,76] always finding good agreement. This is illustrated in what follows for a low lunar frozen orbit. In our simulations we considered a 50th degree truncation of the `LP150Q` model.[77,78] Still the analytical character of the mean elements equations would make easy to change this reference potential, used for the sake of illustration purposes and to ease comparison with previous results in the literature, by more modern Selenopotential determinations.

We fixed the mean semimajor axis to the value of a circular orbit about 100 km above the moon's surface, and use the frozen orbit condition in Eq. (37), to represent the inclination eccentricity diagram in Fig. 1, where the results obtained with the recommended 50th-degree model are superimposed to an analogous curve obtained with a simpler 20th-degree truncation to illustrate the important differences in the frozen orbit condition obtained in the case of high inclination frozen orbits. The detail in the right plot of Fig. 1 shows that there exists an almost circular frozen orbit with a mean inclination of 85 degree, in which we focus in what follows.

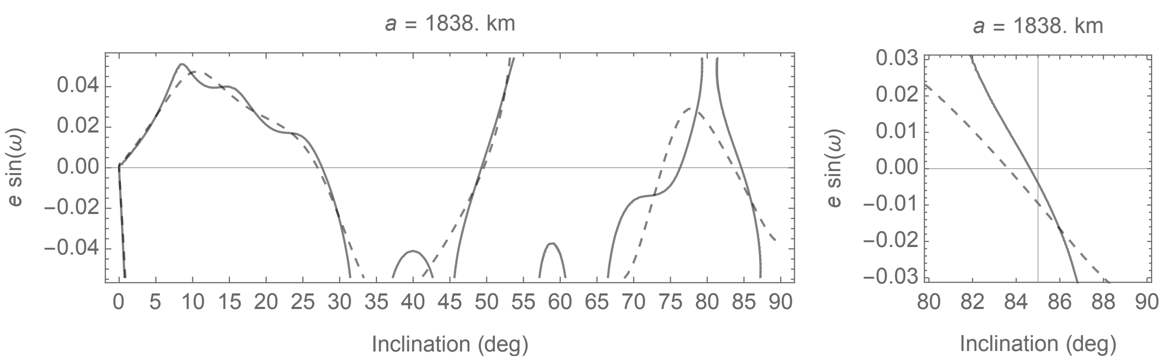

Figure 1. Inclination-eccentricity diagrams of frozen orbits ($\omega = \pm\pi/2$) for an orbiter about 100 km above the lunar surface. Solid line, 50×0 truncation. Dashed line, 20×0 truncation. Right: detail in the region of the higher inclinations. Only non-impact orbits are presented.

A root finding process shows that the exact mean eccentricity of the looked frozen orbit is $e = 0.0039349$ with the mean periapsis frozen at $\omega = 270$ degree. The direct propagation of this orbit in the zonal model using these mean elements as if they were the initial osculating elements is shown in the left column of Fig. 2 for a time propagation interval of three years. It shows that the orbit provided by the mean dynamics is certainly frozen, with bounded long-period oscillations of small amplitude for the eccentricity and argument of the periapsis (second and fourth rows in the left column of Fig. 2), which induce analogous long-period fluctuations in the periapsis distance that range from about 91.5 km to a maximum of 94 km over the lunar surface (bottom plot in the left column of Fig. 2). However, the average values of these oscillations do not match the corresponding

*The periodicity in the orbital plane was originally identified with a periodicity in the rotating meridian plane of the satellite. See, Refs. 71, 72 or §5.5 of Ref. 73.

mean values of the frozen orbit predicted by the analytical theory, not even for the semimajor axis or the inclination, which are only affected of short-period oscillations. The disagreement between the mean and average dynamics is solved when the mean to osculating transformation stemming from the generating function in Eqs. (42)–(43) is applied. Indeed, reducing the semimayor axis by 428 m, decreasing the eccentricity by 0.33 thousandths, and lowering the inclination by just 2 arc seconds, over the mean values, yields initial osculating elements corresponding to the true frozen orbit in the right column of Fig. 2, whose average values are now in perfect agreement with the mean values of the frozen orbit.

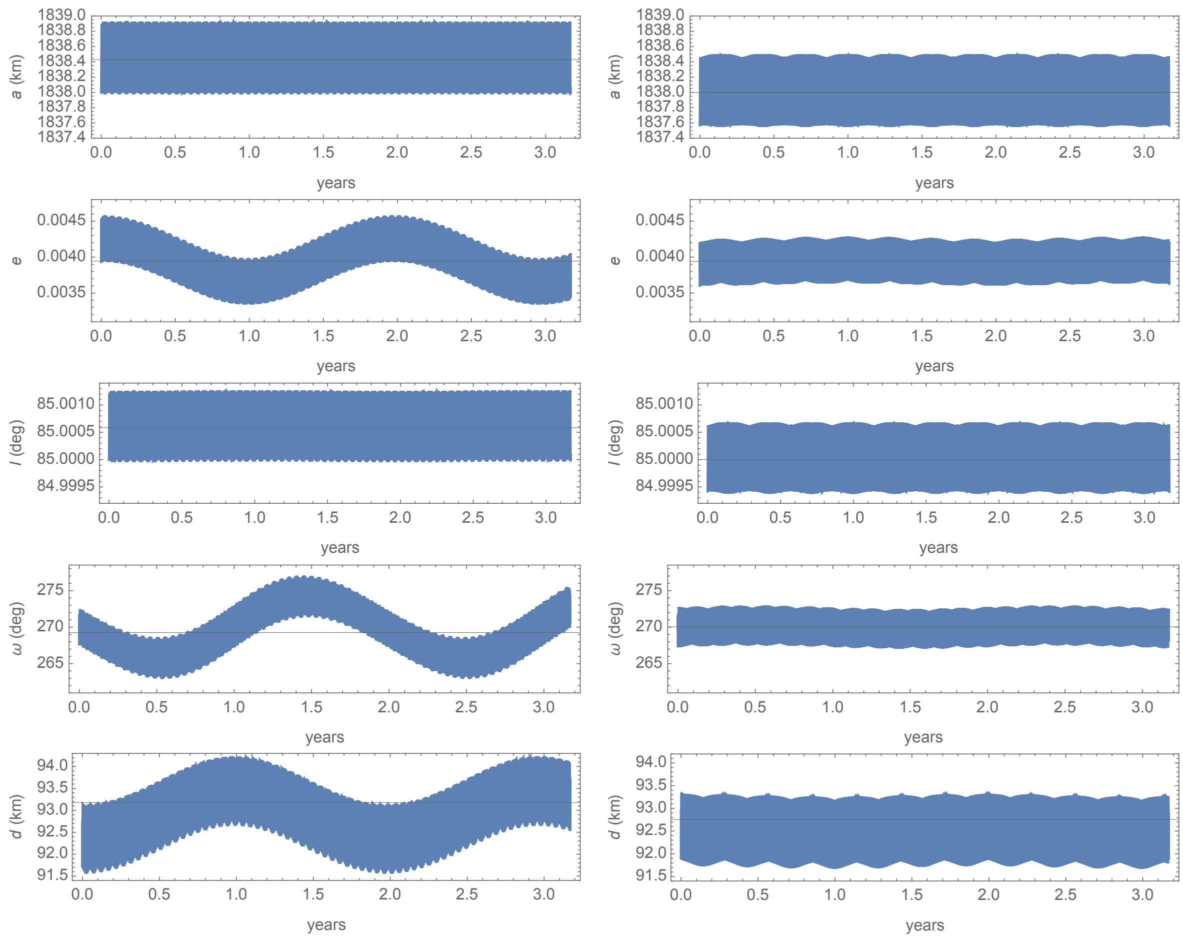

Figure 2. Time history of the orbital elements of the example frozen orbit along a 3-years propagation interval in the non-averaged 50×0 model. Left column: direct propagation of the mean elements. Right column: propagation of initial conditions computed using the mean to osculating transformation.

Figure 3 depicts the evolution of the eccentricity vector in the (moving) orbital plane along the 3-year propagation. The left plot corresponds to the direct propagation of the mean elements in the original, non-averaged model, which confirms that the eccentricity vector remains frozen in the orbital plane, on average, with oscillations of small amplitude over the nominal values. The plot on the right side of Fig. 3 illustrates the radical improvements obtained when the initial osculating elements are corrected with the short-period terms of the theory, and clearly shows the almost periodic character of the frozen orbit in the orbital plane. The lack of exact periodicity is due to the truncation of the perturbation solution to the linear effects, and could be amended with the use of differential corrections, cf. Ref. 79, for instance.

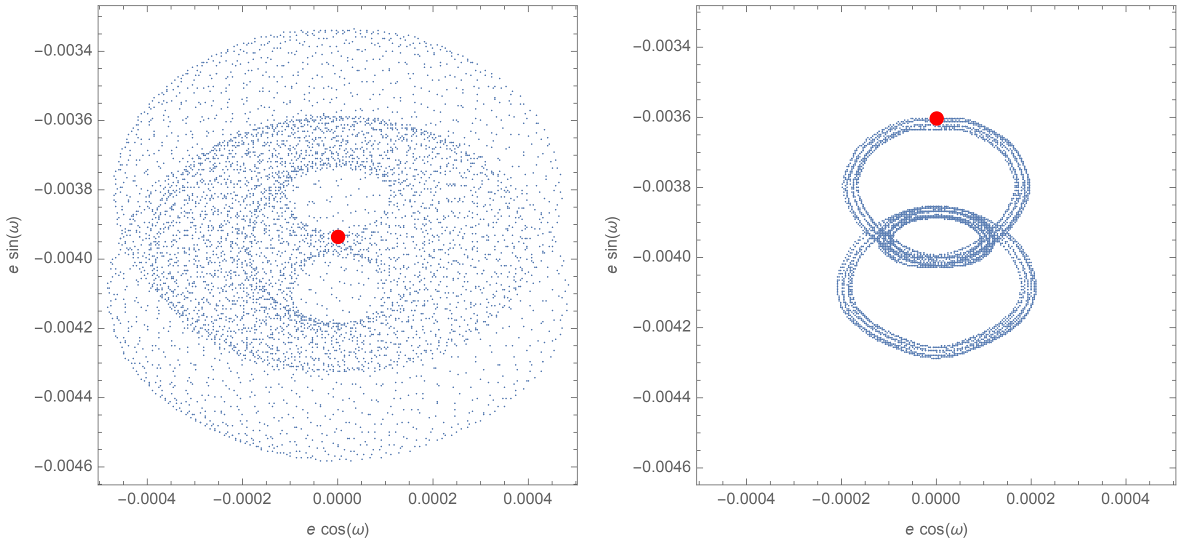

Figure 3. Eccentricity vector evolution in the orbital plane in the 50×0 truncation of the non-averaged zonal model. Left: mean values used as initial conditions. Right: initial conditions from mean values corrected with the short-period terms. Red dots mark starting points of the 3-year propagation

CONCLUSIONS

The use of vectorial formulation for the zonal part of the gravitational potential permitted us to obtain the frozen orbit condition by means of a single scalar equation that is free from geometric singularities, on the one hand, and does not rely on the usual expansions and corresponding truncation of the elliptic motion, on the other hand. Therefore, the new frozen orbit condition is not constrained to the lower eccentricities typical of mapping orbits, which is customary in the literature. In addition, the generating function that allows for the conversion between mean and osculating elements has been derived also in closed form based on the eccentricity and non-dimensional angular momentum vectors. Moreover, the arbitrary integration function of the constant elements of the Keplerian motion, which vary slowly in the case of perturbations, has been determined so that the transformation is purely periodic in the mean anomaly. This is the most favorable condition to connect frozen orbits with (non-averaged) periodic orbits in the orbital plane. Still, the unavoidable truncation of the analytical, frozen orbits obtained in this way could make the use of differential corrections necessary to improve the periodicity in the orbital plane of the frozen orbit in osculating elements. The effect of the tesseral harmonics is not relevant in determining the mean elements of the frozen orbit save for the case of tesseral resonances, and has not been taken into account, yet it may be important in determining the osculating nominal orbit. Future research shall address this case, whose conversion between osculating and mean elements should be achievable also in closed form when approached with known techniques of perturbation methods.

Acknowledgments

Research supported by the Spanish State Research Agency and the European Regional Development Fund (Projects PID2020-112576GB-C22 and PID2021-123219OB-I00, AEI/ ERDF, EU).

REFERENCES

[1] Y. Kozai. The motion of a close earth satellite. *The Astronomical Journal*, 64:367–377, November 1959.

[2] W. M. Kaula. Analysis of Gravitational and Geometric Aspects of Geodetic Utilization of Satellites. *Geophysical Journal*, 5:104–133, July 1961.

[3] W. M. Kaula. *Theory of satellite geodesy. Applications of satellites to geodesy*. Blaisdell, Waltham, Massachusetts, 1966. Reprint: Dover, Mineola, New York, 2000.

[4] E. Cutting, J. C. Frautnick, and G. H. Born. Orbit analysis for Seasat-A. *Journal of the Astronautical Sciences*, 26:315–342, December 1978.

[5] S.-Y. Park and J.L. Junkins. Orbital Mission Analysis for a Lunar Mapping Satellite. *Journal of the Astronautical Sciences*, 43(2):207–217, 1995.

[6] P. Gurfil and M. Lara. Motion near frozen orbits as a means for mitigating satellite relative drift. *Celestial Mechanics and Dynamical Astronomy*, 116(3):213–227, July 2013.

[7] A.S. Konopliv, W.L. Sjogren, R.N. Wimberly, R.A. Cook, and A. Vijayaraghavan. A High Resolution Lunar Gravity Field and Predicted Orbit Behavior (AAS 93-622). In *Advances in the Astronautical Sciences*, volume 85, pages 1275–1295, P.O. Box 28130, San Diego, California 92198, USA, 1994. American Astronautical Society, Univelt, Inc.

[8] M. Lara, S. Ferrer, and B. de Saedeleer. Lunar Analytical Theory for Polar Orbits in a 50-Degree Zonal Model Plus Third-Body Effect. *Journal of the Astronautical Sciences*, 57(3):561–577, July 2009.

[9] S. L. Coffey, A. Deprit, and E. Deprit. Frozen orbits for satellites close to an earth-like planet. *Celestial Mechanics and Dynamical Astronomy*, 59(1):37–72, May 1994.

[10] M. Lara. Exploring Sensitivity of Orbital Dynamics with Respect to Model Truncation: The Frozen Orbits Approach. In M. Vasile, E. Minisci, L. Summerer, and P. McGinty, editors, *Stardust Final Conference*, volume 52 of *Astrophysics and Space Science Proceedings*, pages 69–83, Cham, 2018. Springer International Publishing.

[11] G. W. Rosborough and C. Ocampo. Influence of Higher Degree Zonals on the Frozen Orbit Geometry (AAS 91-428). In B. Kaufman, K. T. Alfriend, R. L. Roehrich, and R. R. Dasenbrock, editors, *Astrodynamics 1991*, volume 76 of *Advances in the Astronautical Sciences*, pages 1291–1304, P.O. Box 28130, San Diego, California 92198, USA, 1992. American Astronautical Society, Univelt, Inc.

[12] R. A. Cook. The long-term behavior of near-circular orbits in a zonal gravity field. In B. Kaufman, K. T. Alfriend, R. L. Roehrich, and R. R. Dasenbrock, editors, *Astrodynamics 1991*, volume 76 of *Advances in the Astronautical Sciences*, pages 2205–2221, P.O. Box 28130, San Diego, California 92198, USA, 1992. American Astronautical Society, Univelt, Inc.

[13] P. d'Avanzo, P. Teofilatto, and C. Ulivieri. Long-term effects on lunar orbiter. *Acta Astronautica*, 40(1):13–20, 1997.

[14] G.-i. Hori. Theory of General Perturbation with Unspecified Canonical Variables. *Publications of the Astronomical Society of Japan*, 18(4):287–296, 1966.

[15] A. Deprit. Canonical transformations depending on a small parameter. *Celestial Mechanics*, 1(1):12–30, 1969.

[16] G. E. Cook. Basic Theory for Prod, a Program for Computing the Development of Satellite Orbits. *Celestial Mechanics*, 7(3):301–314, April 1973.

[17] B. de Saedeleer. Complete Zonal Problem of the Artificial Satellite: Generic Compact Analytic First Order in Closed Form. *Celestial Mechanics and Dynamical Astronomy*, 91:239–268, March 2005.

[18] M. Lara, R. López, I. Pérez, and J. F. San-Juan. Exploring the long-term dynamics of perturbed Keplerian motion in high degree potential fields. *Communications in Nonlinear Science and Numerical Simulations*, 82:105053, March 2020.

[19] V. I. Arnol'd. *Mathematical Methods of Classical Mechanics*, volume 60 of *Graduate Texts in Mathematics*. Springer-Verlag, New York, 2nd edition, 1989.

[20] M. Lara. On mean elements in artificial satellite theory. *Celestial Mechanics and Dynamical Astronomy*, 135(43):1–21, July 2023.

[21] M. Kirschner, O. Montenbruck, and S. Bettadpur. Flight Dynamics Aspects of the GRACE Formation Flying. In *Proceedings of 2nd Workshop on Satellite Constellations and Formation Flying, Haifa, Israel*, 2001.

[22] M. Paskowitz Possner and D. J. Scheeres. Control of Science Orbits About Planetary Satellites. *Journal of Guidance Control Dynamics*, 32(1):223–231, Jan 2009.

[23] M. Lara. On perturbation solutions in the restricted three-body problem dynamics. *Acta Astronautica*, 195:596–604, June 2022.

[24] R. S. Bhat, R. B. Frauenholz, and P. E. Cannell. TOPEX/POSEIDON orbit maintenance maneuver design. In *Astrodynamics 1989*, pages 645–670, January 1990.

[25] Starlink GNC Team. Starlink conjunction avoidance with crewed space stations. SpaceX GNC Memo SAT-51385, SpaceX, Hawthorne, CA, April 2022.

[26] J. R. Guinn. Periodic gravitational perturbations for conversion between osculating and mean orbit elements (AAS 91-430). In B. Kaufman, K. T. Alfriend, R. L. Roehrich, and R. R. Dasenbrock, editors, *AAS/AIAA Astrodynamics Specialist Conference, Durango, CO, Aug. 19-22, 1991*, volume 76 of *Advances in the Astronautical Sciences*, pages 1–25, P.O. Box 28130, San Diego, California 92198, USA, 1992. American Astronautical Society, Univelt, Inc.

[27] E. Wnuk. Prediction of artificial satellite positions on the basis of the second order theory of motion. *Advances in Space Research*, 30(2):321–330, 2002.

[28] B. Strömgren. Formeln zur genaeherten Stoerungsrechnung in Bahnelementen. Angewandt auf die Planeten 633 Zelima, 956 [1921 IW], 979 Ilsewa, 1035 Amata und 1049 [1925RB]. *Publikationer og mindre Meddeler fra Kobenhavns Observatorium*, 65:1–26, January 1929.

[29] S. Herrick. A modification of the "Variation of Constants" method for special perturbations. *Publications of the Astronomical Society of the Pacific*, 60:321–323, October 1948.

[30] P. Musen. Special perturbations of the vectorial elements. *The Astronomical Journal*, 59:262–267, August 1954.

[31] J. F. San-Juan, R. López, and M. Lara. Vectorial formulation for the propagation of average dynamics under gravitational effects (IAC-23,C1,8,3,x78887). In *Proceedings of the 74th International Astronautical Congress (IAC), Baku, Azerbaijan, 2–6 October 2023*, pages 1–10. International Astronautical Federation (IAF), International Astronautical Federation (IAF), 2023.

[32] M. Milankovitch. *Kanon der Erdbestrahlung und seine Anwendung auf das Eiszeitenproblem*. Königlich Serbische Akademie, Belgrade, 1941. English translation: Canon of Insolation and the Ice-age Problem. Israel Program for Scientific Translations, Mechanics of Space Flight series, Jerusalem, 1969.

[33] S. Herrick. Icarus and the variation of parameters. *The Astronomical Journal*, 58:156–164, August 1953.

[34] R. R. Allan and G. N. Ward. Planetary equations in terms of vectorial elements. *Proceedings of the Cambridge Philosophical Society*, 59(3):669, January 1963.

[35] A. J. Rosengren and D. J. Scheeres. On the Milankovitch orbital elements for perturbed Keplerian motion. *Celestial Mechanics and Dynamical Astronomy*, 118:197–220, March 2014.

[36] D. Brouwer. Solution of the problem of artificial satellite theory without drag. *The Astronomical Journal*, 64:378–397, November 1959.

[37] B. A. Ustinov. Motion of Satellites in Small-Eccentricity Orbits in the Noncentral Gravitational Field of the Earth. *Cosmic Research*, 5:159–168, March 1967.

[38] M. C. Eckstein and F. Hechler. A reliable derivation of the perturbations due to any zonal and tesseral harmonics of the geopotential for nearly-circular satellite orbits. Scientific Report ESRO SR-13, European Space Research Organisation, Darmstadt, Federal Republic of Germany, June 1970.

[39] B. J. Cain. Determination of mean elements for Brouwer's satellite theory. *Astronomical Journal*, 67:391–392, August 1962.

[40] H. G. Walter. Conversion of osculating orbital elements into mean elements. *Astronomical Journal*, 72:994–997, October 1967.

[41] S. Spiridonova, M. Kirschner, and U. Hugentobler. Precise mean orbital elements determination for LEO monitoring and maintenance. In *24th International Symposium on Space Flight Dynamics*, pages 1–14, Laurel, Maryland, USA, 2014.

[42] R. H. Lyddane and C. J. Cohen. Numerical comparison between Brouwer's theory and solution by Cowell's method for the orbit of an artificial satellite. *Astronomical Journal*, 67:176–177, April 1962.

[43] J. V. Breakwell and J. Vagners. On Error Bounds and Initialization in Satellite Orbit Theories. *Celestial Mechanics*, 2:253–264, June 1970.

[44] M. Lara. Brouwer's satellite solution redux. *Celestial Mechanics and Dynamical Astronomy*, 133(47):1–20, September 2021.

[45] Y. Kozai. Motion of a lunar orbiter. *Publications of the Astronomical Society of Japan*, 15:301–312, 1963.

[46] B. E. Shapiro. Phase Plane Analysis and Observed Frozen Orbit for the Topex/Poseidon Mission. In P. M. Bainum, G. L. May, Y. Ohkami, K. Uesugi, Q. Faren, and L. Furong, editors, *6th AAS/JRS/CSA Symposium, International Space Conference of Pacific-Basin Societies, Strengthening Cooperation in the 21st Century*, volume 91 of *Advances in the Astronautical Sciences*, pages 853–872, P.O. Box 28130, San Diego, California 92198, USA, 1996. American Astronautical Society, Univelt, Inc.

[47] T. A. Ely. Stable Constellations of Frozen Elliptical Inclined Lunar Orbits. *Journal of the Astronautical Sciences*, 53(3):301–316, 2005.

[48] D. Folta and D. Quinn. Lunar Frozen Orbits. In *AIAA/AAS Astrodynamics Specialist Conference and Exhibit, 21 - 24 August 2006, Keystone, Colorado*, pages 1–18, Reston, Virginia, 2006. American Institute of Aeronautics and Astronautics, Inc. AIAA Paper 2006-6749.

[49] E. Condoleo, M. Cinelli, E. Ortore, and C. Circi. Frozen orbits with equatorial perturbing bodies: The case of ganymede, callisto, and titan. *Journal of Guidance, Control, and Dynamics*, 39(10):2264–2272, 2016.

[50] C. Circi, E. Condoleo, and E. Ortore. A vectorial approach to determine frozen orbital conditions. *Celestial Mechanics and Dynamical Astronomy*, 128(2-3):361–382, June 2017.

[51] S. Kikuchi, Y. Oki, and Y. Tsuda. Frozen Orbits Under Radiation Pressure and Zonal Gravity Perturbations. *Journal of Guidance Control Dynamics*, 44(11):1924–1946, November 2021.

[52] X. Huang, B. Yang, S. Li, J. Feng, and J. J. Masdemont. Design of Ganymede-Synchronous Frozen Orbit around Europa. *Mathematics*, 11(1), 2023.

[53] F. Mignard and M. Henon. About an Unsuspected Integrable Problem. *Celestial Mechanics*, 33(3):239–250, July 1984.

[54] A. Deprit. Dynamics of orbiting dust under radiation pressure. In A. Berger, editor, *The Big-Bang and Georges Lemaître*, pages 151–180, Dordrecht, 1984. Springer.

[55] M. Lara, E. Fantino, and R. M. Flores. Nonlinear effects of the central body oblateness on the coplanar dynamics of solar sails. In *Proceedings of the Third International Nonlinear Dynamics Conference, Rome, Italy, 18–22 June 2023*, NODYCON Conference Proceedings (to appear), pages 1–10, 2023.

[56] M. Lara, A. J. Rosengren, and E. Fantino. Non-singular recursion formulas for third-body perturbations in mean vectorial elements. *Astronomy and Astrophysics*, 634(Article A61):1–9, February 2020.

[57] O. D. Kellogg. *Foundations of Potential Theory*. Dover Publishers Inc., New York, 1953.

[58] D. Brouwer and G. M. Clemence. *Methods of Celestial Mechanics*. Academic Press, New York and London, 1961.

[59] R. H. Gooding. A recurrence relation for inclination functions. *Celestial Mechanics*, 4:91–98, September 1971.

[60] R. H. Gooding and C. A. Wagner. On the inclination functions and a rapid stable procedure for their evaluation together with derivatives. *Celestial Mechanics and Dynamical Astronomy*, 101:247–272, July 2008.

[61] H. Poincaré. *Les méthodes nouvelles de la mécanique céleste. Tome 2*. Gauthier-Villars et fils (Paris), 1893.

[62] Y. Kozai. Second-order solution of artificial satellite theory without air drag. *The Astronomical Journal*, 67:446–461, September 1962.

[63] J. A. Morrison. Generalized Method of Averaging and the Von Zeipel Method. In Raynor L. Duncombe and Victor G. Szebehely, editors, *Methods in Astrodynamics and Celestial Mechanics*, volume 17 of *Progress in Astronautics and Rocketry*, pages 117–138. Elsevier, 1966.

[64] D. Steichen. An averaging method to study the motion of lunar artificial satellites II: Averaging and Applications. *Celestial Mechanics and Dynamical Astronomy*, 68(3):225–247, July 1998.

[65] M. Lara, J. F. San-Juan, Z. J. Folcik, and P. Cefola. Deep Resonant GPS-Dynamics Due to the Geopotential. *Journal of the Astronautical Sciences*, 58(4):661–676, October 2011.

[66] Y. Kozai. Mean values of cosine functions in elliptic motion. *The Astronomical Journal*, 67:311–312, June 1962.

[67] M. Lara and J.F. San-Juan. Dynamic Behavior of an Orbiter Around Europa. *Journal of Guidance, Control and Dynamics*, 28(2):291–297, March-April 2005.

[68] J. F. Palacián, P. Yanguas, S. Fernández, and M. A. Nicotra. Searching for periodic orbits of the spatial elliptic restricted three-body problem by double averaging. *Physica D: Nonlinear Phenomena*, 213(1):15–24, 2006.

[69] M. Lara and J. F. Palacián. Hill Problem Analytical Theory to the Order Four: Application to the Computation of Frozen Orbits around Planetary Satellites. *Mathematical Problems in Engineering*, 2009(Article ID 753653):1–18, 2009.

[70] M. Lara, J. F. Palacián, P. Yanguas, and C. Corral. Analytical theory for spacecraft motion about Mercury. *Acta Astronautica*, 66(7-8):1022–1038, April 2010.

[71] J. M. A. Danby. Motion of a Satellite of a Very Oblate Planet. *The Astronomical Journal*, 73(10):1031–1038, December 1968.

[72] R. A. Broucke. Numerical integration of periodic orbits in the main problem of artificial satellite theory. *Celestial Mechanics and Dynamical Astronomy*, 58(2):99–123, February 1994.

[73] M. Lara. *Hamiltonian Perturbation Solutions for Spacecraft Orbit Prediction. The method of Lie Transforms*, volume 54 of *De Gruyter Studies in Mathematical Physics*. De Gruyter, Berlin/Boston, 1 edition, 2021.

[74] M. Lara, J. F. Palacián, and R. P. Russell. Mission design through averaging of perturbed Keplerian systems: the paradigm of an Enceladus orbiter. *Celestial Mechanics and Dynamical Astronomy*, 108(1):1–22, September 2010.

[75] M. Lara. Design of long-lifetime lunar orbits: A hybrid approach. *Acta Astronautica*, 69(3-4):186–199, August 2011.

[76] M. Lara, B. de Saedeleer, and S. Ferrer. Preliminary design of low lunar orbits. In *Proceedings of the 21st International Symposium on Space Flight Dynamics, Toulouse, France*, pages 1–15. ISSFD, October 2009.

[77] A.S. Konopliv. LP Lunar Gravity V1.0, LP-L-RSS-5-GRAVITY-V1.0. NASA Planetary Data System, 1999.

[78] A. S. Konopliv, S. W. Asmar, E. Carranza, W. L. Sjogren, and D. N. Yuan. Recent Gravity Models as a Result of the Lunar Prospector Mission. *Icarus*, 150:1–18, March 2001.

[79] M. Lara. Fast computation of inclined, frozen, low lunar orbits in a high degree Selenopotential (AAS 10-220). In M. Majji, J. D. Turner, G. G. Wawrzyniak, and W. T. Cerven, editors, *Spaceflight Mechanics 2010*, volume 156 of *Advances in the Astronautical Sciences*, pages 1769–1781, P.O. Box 28130, San Diego, California 92198, USA, January 2010. American Astronautical Society, Univelt, Inc.